International Journal of Adhesion and Adhesives xxx (xxxx) xxx–xxx

Contents lists available at ScienceDirect

International Journal of Adhesion and Adhesives

journal homepage: www.elsevier.com/locate/ijadhadh

Measurement of epoxy film adhesive properties in torsion and tension using tubular butt joints

J. Kosmann[a,*], O. Klapp[b], D. Holzhüter[a], M.J. Schollerer[a], A. Fiedler[b], C. Nagel[b], C. Hühne[a]

[a] DLR – Institute of Composite Structures and Adaptive Systems, Lilienthalplatz 7, 38108 Braunschweig, Germany
[b] Fraunhofer IFAM – Adhesive Bonding Technology and Surfaces, Wiener Straße 12, 28359 Bremen, Germany

ARTICLE INFO

Keywords:
Digital image correlation (DIC)
Contactless biaxial measuring
Epoxides (A)
Destructive testing (C)
Mechanical properties of adhesives (C)

ABSTRACT

With the increasing amount of composite materials used for aircraft structures, structural bonding and bonded repairs are needed. However, a huge challenge is the availability of reliable material properties for the adhesives. A common approach for determining the material properties is to use adhesively bonded tubular butt joint specimens, tested in a biaxial testing system. In order to determine stress-strain curves of the adhesive systems local strain or deformation measurements needs to be performed. But because of the small bondline thickness of an e.g. epoxy film adhesive, the resulting deformations are very small. Within this study, two different strain measurement techniques are used. First a high resolution digital image correlation (DIC) system. Second capacitive sensors combined in a manner, which allows the decoupled measuring of axial and torsional movements. Both methods and results are compared and discussed. Both have their advantages and the ability to measure the small deformations.

1. Introduction

With the increasing amount of composite materials used for civil aircraft structures, joining and repair methods suitable for composite structures are necessary. Possible methods are structural bonding and bonded repairs. However, a huge challenge is the availability of reliable material properties for the adhesives [1–3]. Since the preferred loading of adhesively bonded joints is to be stressed in shear the main interest is to characterize the adhesives shear stress - shear strain behaviour. For high strength structural adhesives systems within the ISO standard 11003-2 single lap joint specimen geometry for shear tests is proposed (Thick Adherends Shear Test, TAST). Due to the short overlap length and the thick adherends the stress concentrations at the overlap ends and the influence to the shear strength are quite small, but still present at the TAST specimen [3]. Alternative specimen geometry for the determination of the adhesives shear stress - shear strain behaviour is an adhesively bonded tubular butt joint following ISO 11003-1. When joining two tubular adherends with the same geometry in terms of inner and outer diameter by means of adhesive butt-wise together, in the intermediate circular ring shaped bondline shear stresses can be introduced by torques acting around the longitudinal axis of the specimen. Due to the circumferential bondline a continuously load flux alongside the bondline is guaranteed so that no stress concentrations occur [3,4]. This enables this specimen type to determine the adhesives shear behaviour very accurate especially in terms of yielding and strength. However, therefore some requirements need to be fulfilled which will be discussed below [5]. In addition the bondline can be stressed not only in shear but also in tension by introducing axial forces in the tubular butt joint specimen [4,6]. By varying the relationship of torque and axial loading arbitrary multiaxial stress states can be generated in the bondline. These results are needed e.g. for the Mahnken-Schlimmer model [7] and for the design of bonded repairs on aircraft primary structures were curved surfaces induce through-thickness stresses as well as shear stresses in the adhesive [8]. By now, for bonded repairs and structural bonded CFRP aircraft structures mostly epoxy film adhesives with a high stiffness and strength and less plasticity are used. Within this study the Henkel Hysol EA9695 AERO 0.05NW film adhesive (Henkel AG&Co., Düsseldorf, Germany) is used. The epoxy film adhesive has a typical cured thickness of 50 to 100 µm. The small thickness and the elevated curing temperature of 130 °C cause manufacturing issues. Thus the tubes are bonded with a new joining device, allowing a pressured and aligned curing in an oven [9]. The thin adhesive between the two bonded adherends means that the occurring deformations for torsion as well as in tension are very small. Furthermore the bonded tubular butt joint configuration allows a multiaxial loading of the specimen type. In order to separate the torsional and axial displacements of the adherends a decoupled measuring of each displacement vector during testing is necessary.

* Corresponding author.
E-mail address: jens.kosmann@dlr.de (J. Kosmann).

https://doi.org/10.1016/j.ijadhadh.2018.02.020

Within this study, two different strain measurement techniques are analyzed and compared. The first is a high resolution digital image correlation (DIC) system. DIC measuring has the advantage of measuring a complete strain field in each direction within the measurement area. The second method relies on contactless working capacitive sensors, combined in a manner, which allows the decoupled measuring of relative axial and torsional movements of the bonded adherends. This method is easy to use and online applicable also to fatigue testing. But it gives only global displacement information. Both methods and results are compared and discussed.

2. Material and methods

2.1. Improved manufacturing of tubular butt joints

As already mentioned above for a multiaxial adhesive characterisation the use of bonded tubular butt joints, under variable torsion and tension loads, is an expedient approach. Important for the quality of the determined material values is the coaxial alignment of the bonded tubes. Also the bondline has to be free of voids and air inclusion. In previous work [5] Wölper investigated the effects of coaxial and angle deviations for the results of material characteristics using FEA. Slight deviations have a strong negative impact to the results. Particularly for thin film-adhesives with elevated curing temperatures, the change of viscosity of the adhesive and the thermal expansion of the tubes must be considered. Previous investigations regarding the manufacturing of the specimens showed shortfalls in joining and curing them [10]. Due to voids, deviations or poorly-bonded tubes, no reliable results could be achieved yet. Therefore, a new joining-device is developed. To bond the specimen both tubes have a separate male and female PTFE core which expands during the increase of temperature in the cure process to the inner diameter of the tubes. Due to an integrated loose fit bearing of the cores, a perfectly coaxial alignment of the tubes is ensured. The separation of the core movement also allows to press the bondline by applying weights on top of the tubes. The constant pressure persists over the whole curing process [9]. The results show well joined tubular specimens without a significant angular and lateral deviation of the adherends. The thickness of the bondline can be adjusted by the weights and is constant over the whole diameter. The new joining-device enables the testing of high quality bonded tubular butt joints to determine the material values of thin elevated-temperature-cured film-adhesive.

2.2. Measuring principle

Within this section the principle of the two different strain measurement techniques are explained. First the high resolution digital image correlation (DIC) system, second the contactless biaxial measuring high resolution extensometer.

2.2.1. High resolution digital image correlation (DIC) system

The first measurement technique investigated within this study is the digital image correlation (DIC). Here the ARAMIS 12M System from GOM GmbH, Braunschweig, Germany is used. As described in previous work [11], it is possible to measure very fine displacements with the right system setup. The DIC measuring has the advantage of measuring a complete strain field in each direction within the measurement area.

2.2.1.1. Parameters. Based on previous work [11] the following setup is used for the undertaken testing. A 3D setup was chosen as there is an out of plane movement of each measuring point during torsional testing. The camera distance and angle is set up for a measurement volume of 24 × 30 mm, which results in an area of 0.16 mm × 0.16 mm for one facet. Using 100 mm lenses, a small aperture and strong light enables a sufficient depth of focus. One more crucial factor for a good measurement is the speckle pattern. Therefore a combination of white titanium dioxide and black iron oxide powder which is dispersed in ethanol and applied with an air brush system was used. In order to calculate the time-depended strain values during a quasi-static test a high frame rate is necessary.

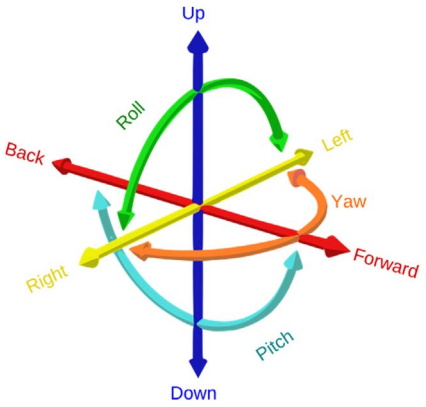

Fig. 1. 6DoF [public domain].

2.2.1.2. Post processing. To gain the necessary data to calculate the material deformation from the DIC measurement several steps are necessary. The evaluation approach within this study is based on local coordinate systems in both adherend tubes. Between this coordinate system the six degrees of freedom (6DoF), see Fig. 1, can be calculated. In here only the up and down movement, which is the axial strain, and the yaw angle for the torsional stain are of interest. Especially the roll and pitch angle should be zero, as a movement in this direction would mean a misaligned testing setup.

Each coordinate system is based on a fitting cylinder over the adherend surface next to the bondline, on a plane normal to the cylinder direction and on a fitting point in the center of the surface, see Fig. 2.

The coordinate system generation based on the fitting elements has the advantage that single facet errors are not critical for the result, but the bigger the fitting area the more adherend strain is cumulated within each fitting point. Furthermore the created local coordinate systems are exactly localised in the middle of the tube and have the right orientation, as shown in Fig. 3, independently of a misaligned camera setup. Without correct referenced coordinate system, the distinction in axial and torsional strain ratios is not possible. The advantage with the calculation of the 6DoF between both local coordinate systems is that the resulting torsional angle and the axial displacement are directly measured on the specimen surface. As shown in Fig. 3 there are two cylinders within each adherend, one next to the bondline and another in some distance to the bondline. This enables to calculate the adherend strains in each tube. Furthermore the axial distance between the supporting fitting points is measured. With both, the adherend deformations can be calculated for each load step. The measured deformation over the adhesive is corrected to obtain the pure adhesive strain.

2.2.2. Contactless biaxial measuring high resolution extensometer

The second measuring method within this study is a contactless biaxial extensometer. Since a main requirement when testing adhesively bonded tubular butt joint specimens under biaxial loading conditions is to measure precisely the expected very small relative displacements (typically in the range of microns). Therefore an appropriate measuring system with a sufficient resolution and accuracy has to be chosen. Another crucial requirement is to reliably decompose the displacement vector of a biaxially loaded, tubular butt joint specimen into its orthogonal components in axial and tangential directions. A third requirement aims at the specification that the measurement shall be performed without significant time delay, such that the test procedure may be controlled based on local displacement data. Furthermore, test data may be obtained in real time in fatigue

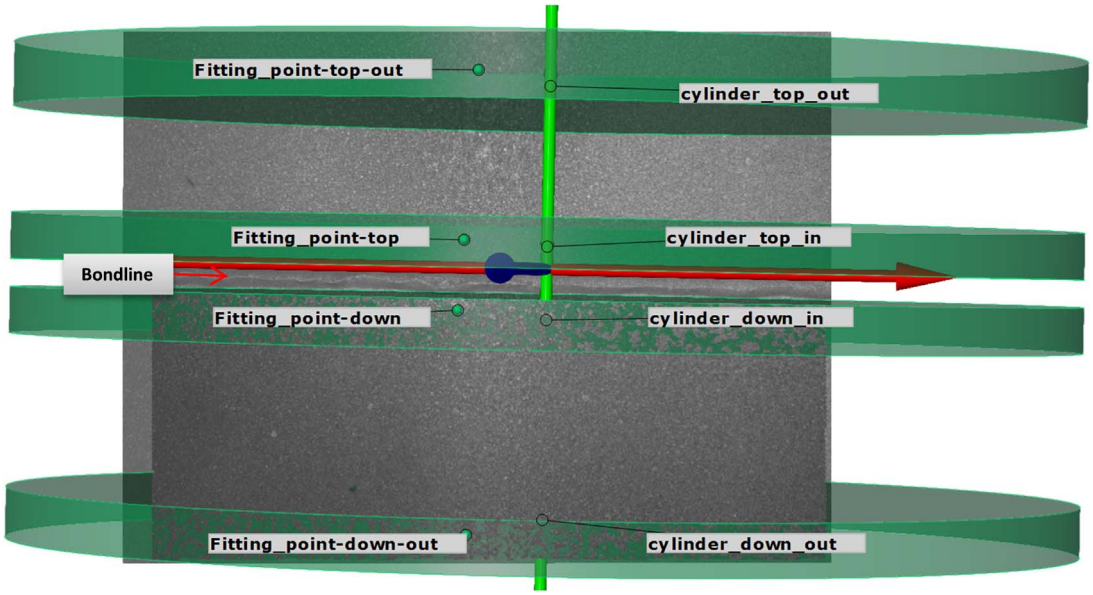

Fig. 2. DIC measurement, illustration of both fitting cylinders one each tube, above and below the bondline.

experiments. The third requirement means, that no extensive post processing of the measured data is necessary. A physical measurement principle which transforms a distance change directly into a voltage output is to measure the capacity of an electric field between an electrode and an opposite conductive metal plate. Since the corresponding areas of the electrode and the plate as well as the dielectric in-between the gap are always the same, a change of the gap width delivers a change of the electrical capacity. By means of an appropriate measuring amplifier, the change of the electrical capacity can be transformed into a linearized voltage output. The chosen capacitive sensors, CSH2FL-CRm1,4 from Micro-Epsilon, Germany, have a measurement range of 0 to 2 mm and a resolution of about 1.5 nm. Due to their high temperature resistance, the sensors may be used in the range from very low temperatures up to 200 °C. The capacitive sensors and corresponding target surfaces have been arranged at the adherend surfaces of a tubular butt joint specimen as schematically shown in Fig. 4. If the specimen is loaded in tension and torsion at the same time, a displacement vector consisting of axial and tangential components exists between two reference points on the upper and lower adherends. Due to the contactless measurement principle, decoupling can be easily achieved by aligning each sensor precisely perpendicular to the target faces. At least two sensors are necessary to perform the desired decomposition.

Since the measurement of the tangential displacement takes place on a circular path with a perpendicular distance of 59 mm from the longitudinal specimen axis, a certain imprecision occurs due to tilting of the measuring and targeting surfaces with increasing rotation angle. Both surfaces are perfectly aligned in the starting position and the maximum expected displacement to be measured is only about 0.2 mm. In this range, the maximum error according to the manufacturer's datasheet is around 0.005% of the measurement range of 2 mm, which leads to a maximum error of approx. $\pm\ 1e-4$ mm. This means that the relative error of a measured tangential displacement of 0.01 mm would be 1%.

As a further consequence of the distance between sensor and sample

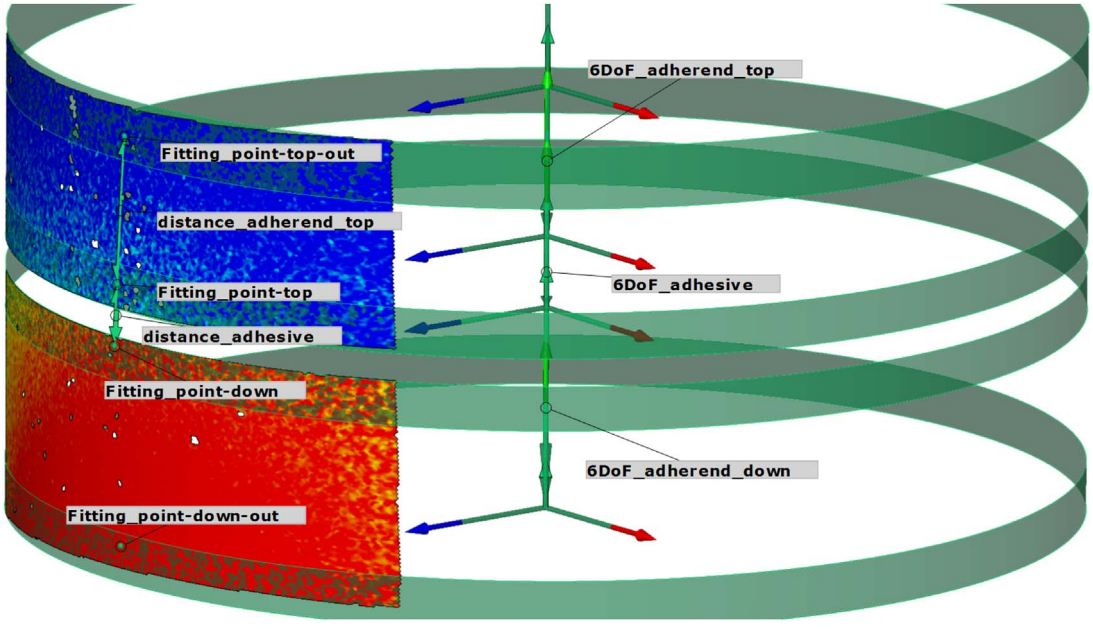

Fig. 3. DIC measurement, fitted local coordinate systems in each cylinder and the calculated 6DoF for each pair.

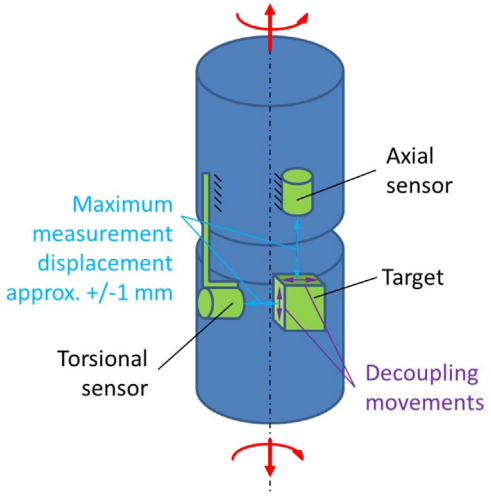

Fig. 4. Arrangement of capacitive sensors for axial and torsional relative displacement measurement.

axis, the measured tangential displacement needs to be recalculated with respect to the position of the sample surface. Since the distances of sample surface and sensor are 30 mm and 59 mm, respectively, the scaling factor is $r_{specimen}/r_{torsial\ sensor} = 30/59$.

In order to fix the sensors and the targeting surfaces at the tubular butt joint specimen, mounting adapters were designed as shown in Fig. 5. The upper mounting adapter, which is hosting the capacitive sensors, is fixed to the upper adherend which is attached to the load cell of the testing machine. The targeting surfaces are incorporated in the lower mounting adapter. This adapter is fixed to the lower end of the specimen into which the axial and torsional loads are introduced. Since there is only a small gap of about one millimeter between the sensor and the targeting surfaces, the torsional loading direction must be chosen such that the gap is increasing with increasing torque. Otherwise it cannot be guaranteed that the threshold monitoring system will stop the cylinder movements in time in order to prevent sensor collision if the sample fails suddenly. When performing fatigue experiments with a stress ratio of R = − 1, no preferred failure direction of the specimen can be determined. Therefore, a defined breaking point was incorporated in the lower mounting adapter such that the targeting surface of the torsional sensor is released in case of a collision movement. It needs to be mentioned that the axial specimen deformation is measured with two sensors on opposite sides of the mounting adapter in order to detect possible secondary specimen deformations. Those secondary specimen deformations might arise due to misalignments of bonded tubular butt joints or misalignments within the load frame of the testing machine.

Another important topic to be considered in order to determine reliable adhesive data is the compensation of the adherend deformation, since the displacement cannot be directly measured at the bondline. Mounting adapters are fixed with a certain distance to the bondline, such that a gap pf 2*3 mm = 6 mm exists between the two opposite, inner edges, as shown in Fig. 5, left. The adherends experience an elastic deformation by the axial and torsional loads, leading to a displacement which is superimposed to the bondline deformation and which depends on the position of the mounting adapters. Since the adapters do not change the adherend stiffness, significant deformation also takes place outside the 6 mm gap in, left. Therefore, one half of the thickness of each mounting adapter (3 mm * 2 = 6 mm, see Fig. 5, right) was considered to contribute to the effective distance, which is finally estimated to be $t_{adh} = 12$ mm.

The adherend displacement can be analytically estimated by the forces acting on the adherends and this material data following Eq. (1) and Eq. (2). The values u_{ax} and u_{tors} must be subtracted from the totally measured axial and tangential displacements, respectively. In order to perform strain-rate controlled tests it is necessary to perform these calculations online in the testing software.

Equation 1		Equation 2	
$\sigma = \frac{F}{A^{CR}} = \varepsilon * E$		$\tau = \frac{M_t}{W_t} = \gamma * G$	
With:		With:	
Normal Stress:	σ	Shear stress:	τ
Force:	F	Torque:	M_t
Area of circular ring:	$A^{CR} = \frac{\pi}{4}*(d_a^2 - d_i^2)$	Elastic section modulus of a circular ring:	$W_t^{CR} = \frac{\pi}{16}\frac{(d_a^4 - d_i^4)}{d_a}$
Outer diameter:	$d_a = 60$ mm	Outer diameter:	$d_a = 60$ mm
Inner diameter:	$d_i = 54$ mm	Inner diameter:	$d_i = 54$ mm
Young's modulus (Steel):	$E = 2.1e5$ MPa	Shear modulus:	$G = \frac{E}{2(1+\nu)}$
Axial strain:	$\varepsilon = \frac{u_{ax}}{t_{adh}}$	Poisson's ratio (Steel):	$\nu = 0.3$
Axial displacement:	u_{ax}	Shear strain:	$\gamma = \frac{u_{tors}}{t_{adh}}$
		Torsional displacement:	u_{tors}
Effective axial adherend length:	t_{adh}	Effective torsional adherend length:	t_{adh}
$\rightarrow u_{ax} = \frac{F * t_{adh}}{A^{CR} * E}$		$\rightarrow u_{tors} = \frac{M_t * t_{adh}}{W_t * G}$	

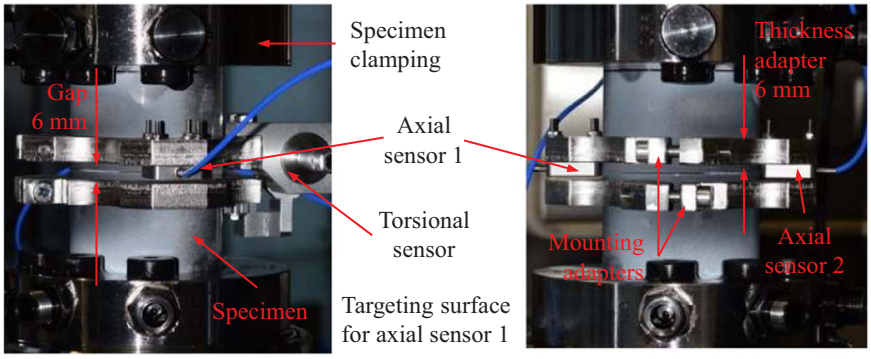

Fig. 5. Mounting adapter with capacitive sensors and targeting surfaces.

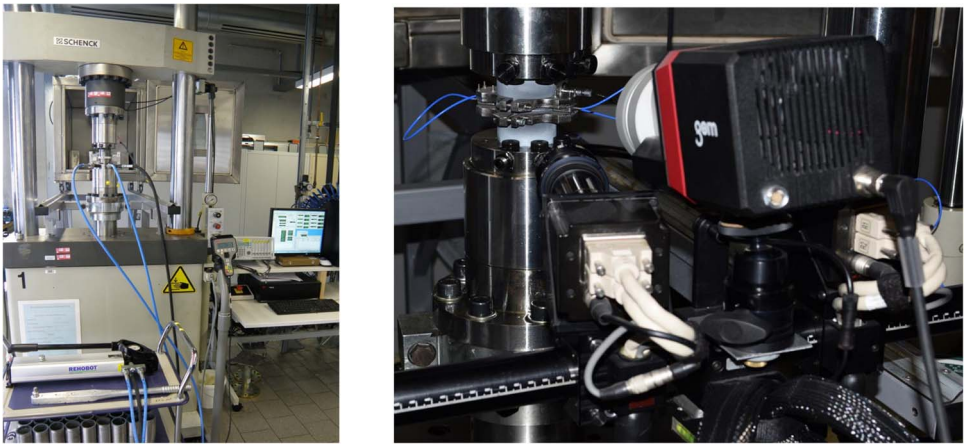

Fig. 6. Test set up: biaxial tension/torsion testing machine (left), extensometer and DIC system (right).

2.3. Testing machine

In order to test the application of the DIC system and the biaxial extensometer for measuring the bondline deformation of an uni- and biaxially loaded adhesively bonded tubular butt joint specimen, a preliminary test campaign has been conducted. To compare the two measurement systems, both systems are used simultaneously for selected specimens. For loading the specimens, a servo-hydraulic biaxial tension/torsion testing machine from Schenck, Germany, (Fig. 6, left) was used. It has a digital controlling unit and a maximum static loading capacity of 250 kN and 1000 N m. The tests were conducted at room temperature controlling the piston's position with a constant axial rate of 1e−3 mm/s and a torsional rate of 1e−2 °/s, respectively. For clamping the tubular specimen, the testing machine is equipped with hydraulic grips. All relevant test data including the sensor data from the extensometer were acquired and recorded by the controlling unit. In addition these data were sent online to the DIC system for storage. The detailed test set up used for measuring the specimen deformation with the DIC system and the biaxial extensometer is shown in Fig. 6, right.

3. Results

In the following the measurement results of selected specimens determined with the DIC system and the biaxial extensometer are discussed. For this study four specimens have been analysed. Specimen v06 and V09 are loaded torsionally, V10 axially and V13 with a combined load.

3.1. Contactless biaxial measuring high resolution extensometer

In Fig. 7 the test data of an adhesively bonded torsionally loaded tubular butt joint specimen is plotted as a function of test time. After 10 seconds of testing time the angle measurement as well as the torque measurement show some noise which can be explained by a temporary malfunction of the torque piston of the used testing machine (same at Fig. 10) which needs to be fixed before continuing the test campaigns. As can be seen in this plot the rotation angle is increasing linearly with time until the specimen failed after about 60 s. The measured torque at this moment is about 800 Nm. Since the movement of the axial piston is not restricted, no axial force may affect the test. The dashed blue line represents the torsional displacement of the biaxial extensometer, already recalculated to the specimen's outer diameter of 60 mm. Subtracting the adherend deformation from this data leads to the solid blue line which is assumed to be the relative torsional displacement of the adherends close to the bondline. This displacement is during a wide range of the test time below a value of 5 µm. Just at the end of the test when the plastic deformation of the adhesive bondline has started this

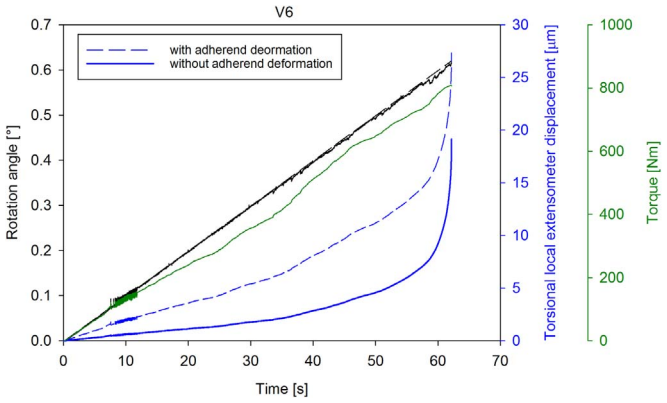

Fig. 7. Test data vs. time for an adhesively bonded and torsionally loaded tubular butt joint specimen (V6).

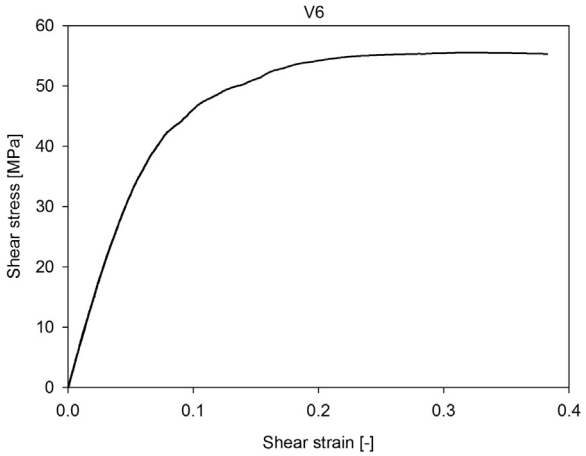

Fig. 8. Shear stress plotted vs. shear strain for the adhesively bonded and torsionally loaded tubular butt joint specimen (V6).

torsional displacement increased immediately up to nearly 20 µm.

Using the formulas given in Eq. (2) and a determined bondline thickness of 50 µm, the shear stress and shear strain can be calculated and plotted as shown in Fig. 8.

An adhesive shear strength of about 55 MPa can be determined from the stress-strain curve. Yielding starts at about 30 MPa and the shear modulus determined up to this nearly linear range is about 670 MPa.

In Fig. 9 the test data of an axially loaded tubular butt joint specimen is plotted vs. the test time. The piston displacement is increasing linearly with time until the specimen failed after nearly 70 s at about

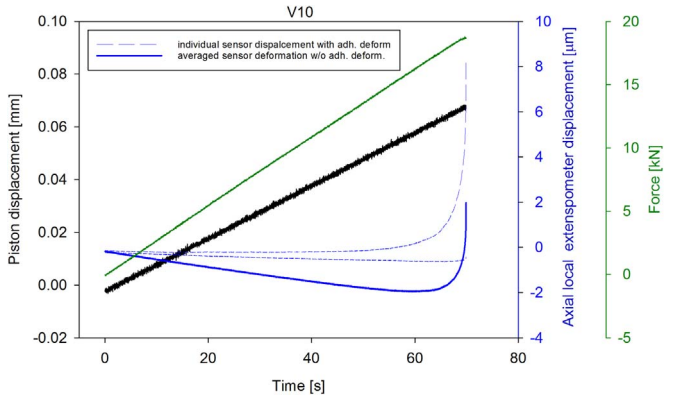

Fig. 9. Test data vs. time for an adhesively bonded and axially loaded tubular butt joint specimen (V10). (For interpretation of the references to color in this figure, the reader is referred to the web version of this article.)

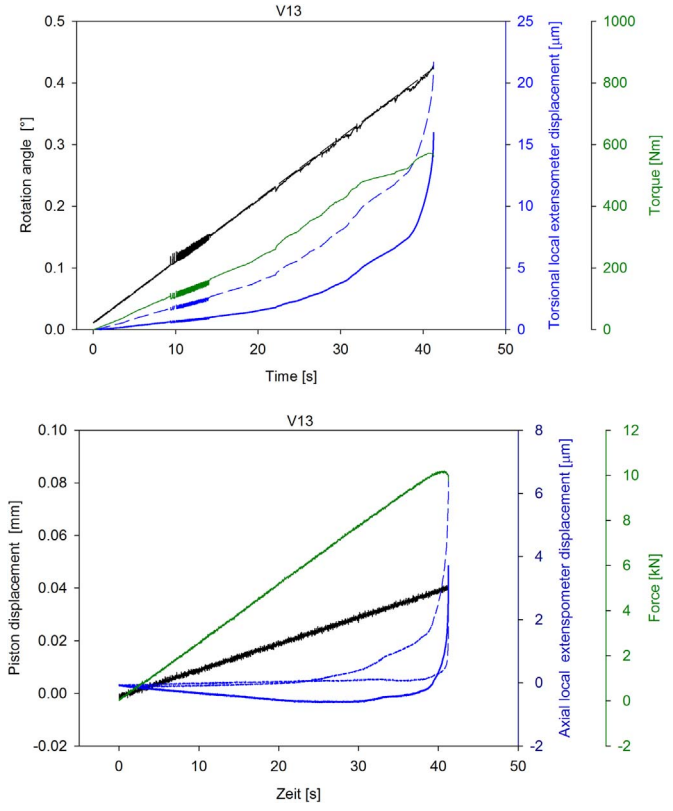

Fig. 10. Test data vs. time for an adhesively bonded and biaxially loaded tubular butt joint specimen (V13), above: torsional data, below: axial data. (For interpretation of the references to color in this figure, the reader is referred to the web version of this article.)

19 kN. The two thin dashed blue lines represent the two individual axial sensor displacements of the biaxial extensometer. It can be noticed that both of them show a very small decreasing negative displacement over the testing time up to − 0.5 µm, which means that the two adherends should approach each other. However, this finding is at the first look in contradiction with the steadily increasing tensile load. It might be a strong hint that the axial load path is not perfectly aligned since the specimen coaxiality is found to be good. Subtracting additionally the load dependent adherend deformation from the averaged displacement leads to the thick solid blue line which is assumed to be the relative axial displacement of the adherends close to the bondline. Since the base data as well as the averaged displacement are negative, the analytical correction of the adherend deformation considering the positive tensile load leads to a further reduction of the determined relative axial

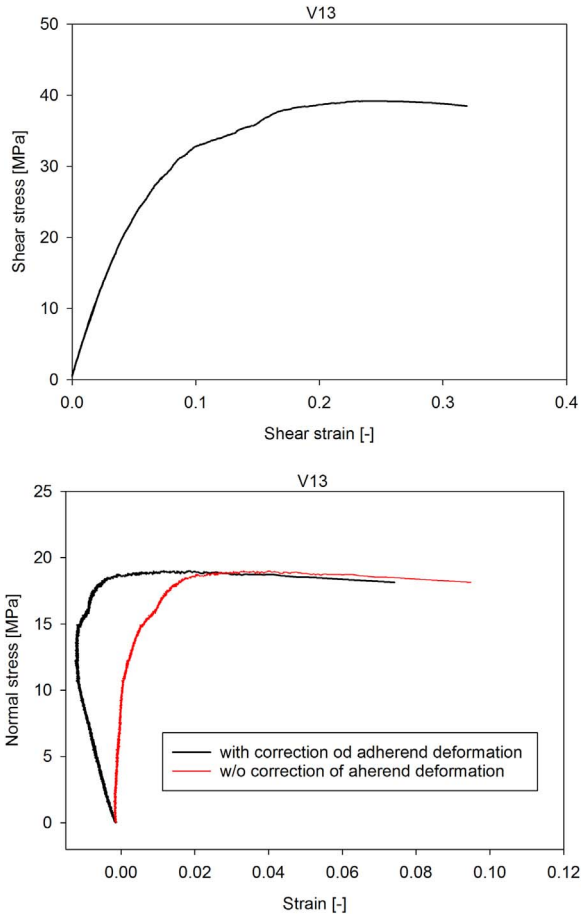

Fig. 11. Stress plotted vs. strain for the biaxially loaded tubular butt joint specimen (V13), above: shear stress - shear strain curve, below: normal stress – strain curve.

displacement. This averaged and corrected displacement is during a wide range of the test time negative up to − 1.9 µm at 60 s testing time. Only at the very end of this tensile test when yielding and plastification takes place, a small positive averaged displacement of about 2 µm can be determined. As already said before, these findings are a clear hint to review once more critically the alignment of the test setup.

In Fig. 10 the test data of a biaxially loaded tubular butt joint specimen is plotted vs. the test time. The specimen failed after about 41 s at about 580 Nm and 10 kN. In comparison to the purely torsionally and axially loaded specimens, these values are clearly reduced due to the multiaxial loading. Also the locally measured and corrected torsional displacement is slightly reduced in comparison to the pure torsion test. However, analyzing the axial data the same issue can be noticed as already found for the pure axial tensile test. For 25 s of the testing time both axial sensors of the extensometer did not measure any significant relative displacement of the adherends. Afterwards, only one axial sensor is measuring a continuously increasing displacement while the other sensor stays mostly unaffected until to the very end of the test. Just 3 s before plastic deformation takes place (which can be seen by the force reduction) also the second axial sensor measures a positive displacement signal. Although the averaged displacement is a small positive value, the correction for the adherend deformation leads again to a negative (compression) displacement.

The resulting stress-strain plots for the torsional as well for the axial loading direction are shown in Fig. 11. For the shear behaviour of the multiaxially loaded adhesive a shear strength of approx. 40 MPa is determined. Yielding starts somewhere between 10 and 20 MPa and a shear modulus of 500 to 600 MPa in the elastic region before can be estimated by a detailed look on the result. For the tensile behaviour of

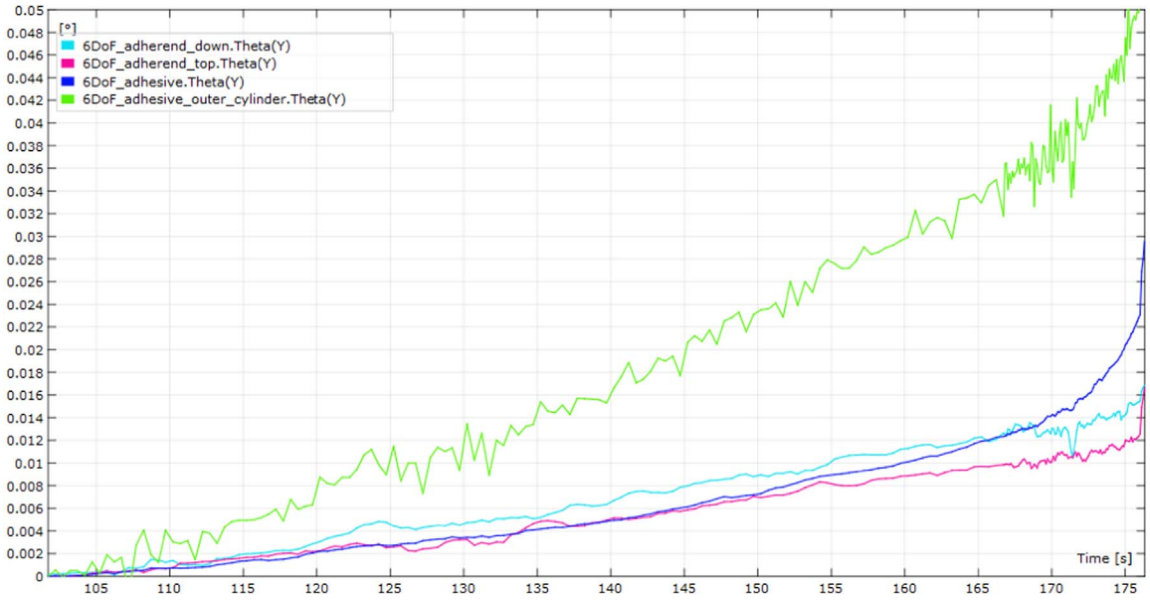

Fig. 12. Test data vs. time - Influence of adherend strain on the torsional measurement. (For interpretation of the references to color in this figure, the reader is referred to the web version of this article.)

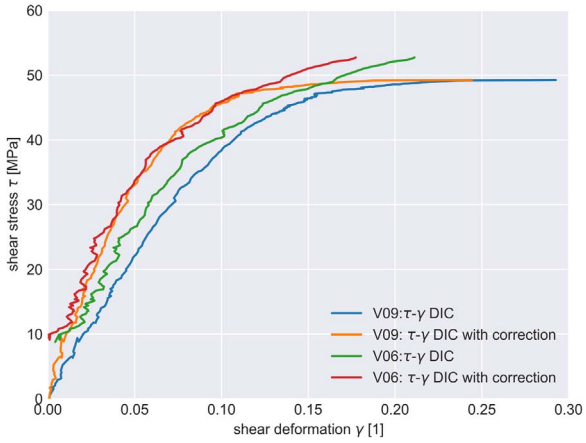

Fig. 13. Shear stress vs. shear strain for both DIC measurements, with and without adherend compensation. (For interpretation of the references to color in this figure, the reader is referred to the web version of this article.)

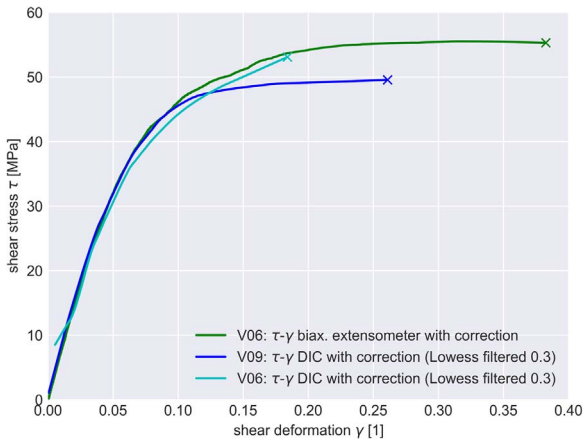

Fig. 14. Shear stress vs. shear deformation for both measurement systems, with adherend compensation and lowess filter. (For interpretation of the references to color in this figure, the reader is referred to the web version of this article.)

the multiaxially loaded adhesive, a yielding limit of about 10 MPa can be determined. Afterwards plastification takes place and nominal normal tensile strength of approx. 19 MPa can be determined before the adhesive failed at about 10% failure strain. The determination of the axial stiffness depends strongly on the measured strain and local axial displacement, respectively, which is still an issue at this moment. Without taking into account the adherend deformation the evaluation of the red stress-stain curve (Fig. 11, below) leads to an axial adhesive modulus of about 22.8 GPa which is not plausible, even if the restricted transvers strain of the adhesive in the bondline is considered. On this account further investigations are necessary, but the capacitive measuring shows that it is possible to measure this small deformation even if there are still issues with the testing machine.

3.2. High resolution digital image correlation (DIC) system

To discuss the DIC results pure torsional loaded specimens were analysed within this work due to the issues with the axial alignment of the test setup. Here two specimens were tested, one only with the DIC System (V09) and one with both systems (V06).

To validate the measurement the first evaluation was performed on the purely DIC measured specimen. In Fig. 12 the torsional angle over the test time is plotted. The light blue and red lines show the torsional angle within each adherend. The torsional angle over the bondline is plotted with the dark blue line, calculated with the inner cylinders, and in green, calculated with the outer cylinder. In order to see the real measurement capabilities the results are not smoothed or filtered in this first step.

It can be seen that the results show some random noise, but the system resolution is good enough to measure the occurring deformations. Comparing the green and the dark blue line it is crucial for the results to consider the adherend deformation. The adherend deformation is plotted with the light blue and red lines for each tube half. The next step is to normalise the displacement with the distance between the anchor points and calculate the correction for the adherend displacement. The measurement confirms the in Equation 2 assumed linear behavior of the adherends. Furthermore the measured correction factor correlates with the analytical calculated factor. For the specimen V06 with both measuring systems, the DIC measurement was performed in the gap between the mounting adapters. Thus only the two inner cylinders can be measured. The adherend deformation correction is

Table 1
Comparison of both measuring systems.

3D DIC	Biaxial extensometer
+ Adherend deformation is measured at each time	− No direct measuring of adherend deformation
+ single set up time is short	− Precise clamping is necessary (first version of mounting adapters have an undefined clamping area)
− Quality of measuring is dependent form calibration	
− Measurement needs post processing	+ Measuring results are online in testing machine available
− Measuring results showing some random noise	+ Good signal quality
− High frequency results in big data	+ High measurement frequency is possible
− Hot/wet and decreased temperature measurements only through window possible	+ Measurement under hot/wet and decreased temperature conditions are possible

taken from the V09 specimen. Furthermore the area for the fitting point was smaller which leads into more random noise. Fig. 13 plots the shear stress vs. shear stain for both DIC measurements one without adherend correction, blue and green, and with the measured correction, in red and orange. It has to be mentioned that the fitting point distance for V06 and V09 is different so the green and blue line including a different amount of adhesive deformation. Furthermore the DIC measuring of V06 stated later so there are missing values in the beginning. But it can be seen, that the corrected stress-strain curves fits together up to 48 MPa of shear stress. From there the V06 specimen increases a bit more and V09 stays on a constant stress level. The determined failure shear strain of specimen V09 is instead of that clearly higher.

3.3. Comparison

To compare both measuring systems, the results measured with the biaxial extensometer and with the DIC system are shown in Fig. 14. The biaxial extensometer results for specimen V06 are plotted in green, the light blue line shows the same specimen measured with DIC and the blue line is the purely DIC measured specimen. Comparing the DIC results, it can be seen that the stiffness of the two samples compares well and the deviation of the two maximum shear stresses from the mean value is well within 5%, which would be expected for this type of structural adhesive. The DIC measurement of V06 started somewhat later than the torsion test, which results in a difference of the two curves close to the origin. The DIC measurement of V06 ends at a shear strain of 0.18 while V09 shows a value of 0.26. Although the deviation of the two values from the average is within 20%, which is typical for structural adhesives, there is another reason for the deviation: Specimen V06 was measured using a sampling rate of 2 Hz for the generation of the digital images, while a frequency of 10 Hz was used for specimen V09. In both experiments, test data had been Lowess filtered in order to get a smooth signal. In the test of specimen V06, the last calculated DIC step for was 0.4 s before the specimen failed. Since plastic deformation of the adhesive started shortly before the specimen failed, the sampling rate of the DIC System was too low in order to reproduce the correct shear strain after Lowess smoothing. Due to the higher sampling rate in the V09 test, a higher shear strain rate was calculated after Lowess smoothing as compared to V06. Comparing the DIC and extensometer results, it can be seen that both measurement techniques give almost identical stiffness results. The difference between the maximum shear stress values in the V06 test is a consequence of the low sampling rate in the DIC measurement. The maximum shear stress difference between V09 DIC and V06 extensometer tests can be explained by natural scatter which is to be expected between different specimens. Due to the higher sampling rate, the maximum shear strain of 0.26 as measured by DIC in the V09 test is more accurate than in the V06 test. Comparing this value with the value of 0.38 as measured by extensometer in the V06 test, a deviation below 20% from the mean can be estimated. Deviations of up to 20% are typically found in the maximum shear strain as measured in structural adhesive torsion tests.

4. Conclusion

The aim pursued within this study was the measurement of epoxy film adhesive properties in torsion and tension using adhesively bonded tubular butt joint specimens. Therefore a DIC system and a contactless working biaxial extensometer with capacitive sensors were used. Both systems prove within a first test campaign in principle their suitability. While the issues for the DIC system are widely related to the correct application of the system to the special application case, the issues to be cleared for the biaxial extensometer were how to decouple the both measurement directions, selection of suitable sensors with sufficient resolution and accuracy, and the mounting to the tubular specimen. The measurement results for both systems clearly show that measuring with digital image correlation as well as the biaxial extensometer is suitable for the adhesively bonded tubular butt joints with epoxy film adhesives. Both systems offer specific benefits, shown in Table 1. One important outcome of this first test campaign is that the displacements to be reliably measured when testing adhesively bonded tubular butt joint specimens are in the low micron range. The sensors installed in the biaxial extensometer fulfil these requirements very well. For the application and use of the biaxial extensometer within axial loading experiments, the observed issues regarding the small axial displacements have to be cleared. This might be not only an issue of the extensometer, but also of the correct alignment of the testing machine and the alignment of the tubular butt joint specimens itself.

Acknowledgements

This work was undertaken within the FACTOR project (20W1520F) funded by the German Ministry of Commerce. The authors would like to thank the DLR for providing the ARAMIS System, the Fraunhofer IFAM for testing the specimens and developing the biaxial extensometer and company GOM for support with the DIC evaluation.

References

[1] Budhe S, Banea MD, de Barros S, da Silva L. An updated review of adhesively bonded joints in composite materials. Int J Adhes Adhes 2017;72:30–42.
[2] Banea M, da Silva L. Adhesively bonded joints in composite materials: an overview. Proc Inst Mech Eng Part L: J Mater Des Appl 2009;223:1.
[3] da Silva L. Failure strength tests. In: Lucas F, da Silva M, Öchsner A, Adams RD, editors. Handbook of adhesion technology. Heidelberg: Springer; 2011.
[4] Engasser I, Puck A. Zur Bestimmung der Grundfestigkeiten von Klebverbin-dungen bei einfacher und zusammengesetzter Beanspruchung. Kunststoffe 1980;70:423–9.
[5] Wölper J, Löebel T. Untersuchungen von Torsionsproben zur Kenndatenermittlung von Klebstoffen mit Hilfe der Finiten Elemente Methode (FEM). Braunschweig: DLR; 2015.
[6] Maibaum D. Mechanisches Verhalten von Metallklebverbindungen bei ein- und mehrachsiger Kurz- und insbesondere Langzeitbeanspruchung. Paderborn: Dissertation Universität Gesamthochschule Paderborn; 1990.
[7] Rolf M, Schlimmer M. Simulation of strength difference in elasto-plasticity for adhesive materials. J Num Met Eng 2005;63:1461–77. http://dx.doi.org/10.1002/nme.1315.
[8] Wang CH, Chalkley P. Plastic yielding of a film adhesive under multiaxial stresses. Int J Adhes Adhes 2000;20:155.
[9] Schollerer MJ, Kosmann J, et al. A new joining-device for manufacturing tubular butt joints with higher curing temperatures of film adhesives. Appl Adhes Sci

2017;5:15. http://dx.doi.org/10.1186/s40563-017-0094-8.
[10] Ehmke S, Kosmann J, et al. Analyse und Charakterisierung der produktionstechnischen Einflüsse bei der Herstellung von Rohrprüfkörpern für multiaxiale Versuche zur Ermittlung zuverlässiger Festigkeitswerte von Filmklebstoffen. andere. DLR-Interner Bericht. DLR-IB 131-2015/43; 2015.
[11] Kosmann J, Löbel T, et al. High resolution digital image correlation strain measurements of adhesively bonded joints. In: Proceedings of the ECCM17 − 17th European Conference on Composite Materials, Munich; 2016.